Bull. Soc. R. Sci. Liège, 2024, **93**(3), 283–290 *Peer-reviewed conference paper*
doi:10.25518/0037-9565.12355

X-ray Microcalorimeter Observations of High-mass X-ray Binaries with the *Resolve* Instrument Onboard *XRISM*

Pragati PRADHAN[1,*] and Masahiro TSUJIMOTO[2,*]

[1] Physics and Astronomy Department, Embry–Riddle Aeronautical University, 3700 Willow Creek Road, Prescott, Arizona, USA
[2] Institute of Space and Astronautical Science (ISAS), Japan Aerospace Exploration Agency (JAXA), 3-1-1 Yoshinodai, Chuo-ku, Sagamihara, Kanagawa 252-5210, Japan
[*] Corresponding authors: pradhanp@erau.edu, tsujimoto.masahiro@jaxa.jp

Paper presented at the 41st Liège International Astrophysical Colloquium on "The eventful life of massive star multiples," University of Liège (Belgium), 15–19 July 2024.

Abstract

The X-ray Imaging and Spectrometer Mission (*XRISM*) was put into orbit successfully in September 2023. *Resolve*, one of the scientific instruments onboard *XRISM*, hosts an X-ray spectrometer based on X-ray microcalorimetery technology. It excels in high spectral resolution, a large throughput, a large bandpass, low background, and good timing accuracy. These properties are suited to bring new insights especially in high-mass X-ray binaries (HMXB). We describe these unique features of *Resolve* and present initial highlights of two HMXB sources.

Keywords: high energy astrophysics, X-ray binary stars, neutron stars, individual (Vela X-1, Cen X-3)

Résumé

Observations de binaires X à forte masse au microcalorimètre à rayons X avec l'instrument *Resolve* à bord de XRISM. La mission *XRISM* (*X-ray Imaging and Spectrometer Mission*) a été mise en orbite avec succès en septembre 2023. *Resolve*, l'un des instruments scientifiques à bord de *XRISM*, héberge un spectromètre à rayons X utilisant la technologie de la microcalorimétrie. Il possède une très haute résolution spectrale, un débit important, une large bande passante, un faible bruit de fond ainsi qu'une très bonne précision temporelle. Ces propriétés nous permettent d'obtenir de nouvelles informations, en particulier pour ce qui concerne les binaires X à forte masse (HMXB). Nous décrivons ci-dessous les caractéristiques uniques de *Resolve* et présentons les premiers résultats de deux HMXBs.

Mots-clés : astrophysique des hautes énergies, étoiles binaires X, étoiles à neutrons, étoiles individuelles (Vela X-1, Cen X-3)

1. Introduction

High-mass X-ray binaries are comprised of compact objects (neutron stars and black holes) and an early-type star with a mass of $\gtrsim 10 M_\odot$. They are rare (100–200 known; the latest is currently updated at https://binary-revolution.github.io/HMXBwebcat/index.html) but constitute the brightest end of X-ray sources in our Galaxy. They are important in many astrophysical contexts, including the mass accretion onto compact objects, UV line-driven winds under the intense X-ray radiation field, and binary evolution toward double compact binaries for eventual gravitational wave sources. Revealing the velocity and density distribution of the system is what observations can deliver to constrain theories. In HMXBs, X-ray emission from the compact object can penetrate through these materials whose distributions are convolved in profiles of emission and absorption lines. High-resolution X-ray spectroscopy is a vital tool for the study of HMXBs. The field is expected to make a giant leap with the advent of X-ray microcalorimeter spectrometer *Resolve* onboard the *XRISM* satellite launched in 2023 September. We describe its unique features in Sect. 2 and present some of the initial results in Sect. 3.

2. *Resolve*

Resolve [1] is one of the two scientific instruments onboard the *XRISM* satellite [2]. It is based on the X-ray microcalorimetry with 6×6 pixels consisting of an HgTe X-ray absorber and Si thermistor. The energy deposited by individual X-rays with ~ 1 fJ increases the temperature by ≈ 1 mK of the ion-doped Si thermistor thermally anchored to the 50 mK stage. The cold stage is maintained by the multi-stage cooling chain consisting of adiabatic demagnetization refrigerators (ADRs), mechanical coolers, and superliquid He in the cryostat.

Resolve has several advantages over the existing technologies (e.g., high-energy transmission grating spectrometer HETG onboard the *Chandra* X-ray observatory [3]) for the studies of HMXBs. First, it has a spectral resolution $R \equiv E/\Delta E \simeq 1300$ at the Fe K-band (cf. $R \simeq 167$ for HETG), which allows us to resolve the fine-structure of He-like Fe K lines useful for various diagnostics of the high-temperature plasmas. Second, it has a large effective area $A_{\rm eff}$ of about $180\,{\rm cm}^2$ at 6 keV (cf. $A_{\rm eff} \simeq 20\,{\rm cm}^2$ for HETG). The effective area mentioned here at 6 keV is already factoring in the closed gate valve configuration. The gate valve is an X-ray transmissive window to keep the cryostat leak-tight before the launch. It is intended to be opened in the orbit, but the opening procedure has not been successful so far. This led to a suppression of all the sensitivity of resolve below roughly 2 keV and a substantial reduction of the effective area at higher energies.

This allows us to take well-exposed spectra as a function of the orbital phase. Third, the energy determination accuracy is high to $\delta E \lesssim 1$ eV due to the onboard energy calibration sources intermittently used during observations (Fig. 1). This allows us to track the radial velocity of $\lesssim 50$ km s^{-1} sufficient for the binary orbital and proper motions. Fourth, the time tagging accuracy of X-ray events is very high ($\delta t \sim 80\,\mu$s) compared to CCD-based spectrometers. This enables spin-phase resolved high-resolution X-ray spectroscopy of pulsars. Finally, the background level is low only of one background event per spectral bin per a 100 ks exposure. This

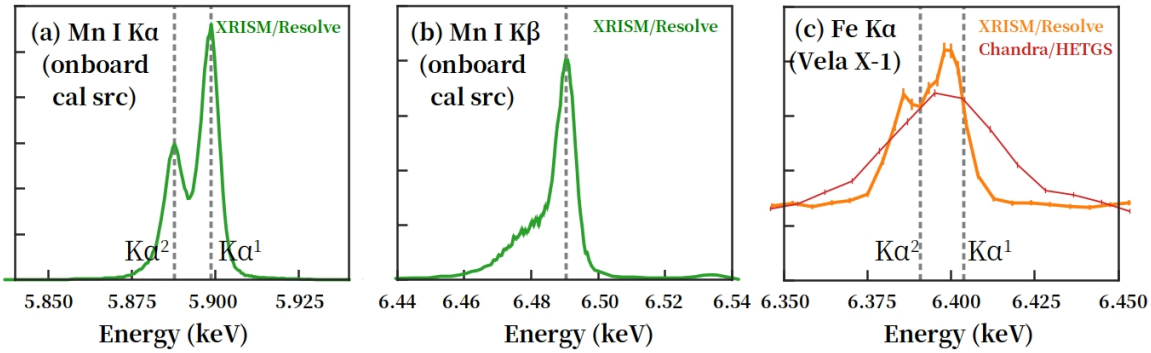

Figure 1: *Resolve* spectrum of (a) Mn I Kα at 5.9 keV and (b) Kβ at 6.4 keV of the onboard calibration source compared to (c) Fe Kα at 6.4 keV of Vela X-1 in the same 20 eV width. The line centroid is redshifted significantly thanks to the energy determination accuracy of the order of 0.1 eV.

allows to detect continuum photons at a high S/N, hence to characterize the absorption line profiles better than previously running and currently operating instruments.

3. Initial Results of HMXBs

3.1. Vela X-1

Vela X-1 (4U 0900-040) is an eclipsing HMXB, where the neutron star is spinning at a period of 283 s and accretes matter from the companion's stellar wind [4]. The orbital period of the system is 8.9 d and is located 2 kpc away [5]. The system's high inclination ($> 73°$; [6]) makes it an excellent candidate for studying accretion and wind characteristics by observing changes at various orbital phases (e.g., [7, 8]). When measured across multiple cycles, it was found that absorption varies predictably, with minimum after eclipse, around phase 0.3, then gradually increases, with a marked spike near phase 0.5 [9]. However, measurements of absorption at the same phase often differ from one orbit to another [10]. Additionally, the distribution of phase-averaged brightness in Vela X-1 deviates from the expected log-normal pattern, likely due to the system's complex and chaotic accretion flow [8], as exhibited also by its extreme X-ray variability, including giant flares and off states. The X-ray spectrum features lines of He-like ions and a strong 6.4 keV iron line (see [11] and references therein).

Vela X-1 was observed with *XRISM* as a part of the performance verification program covering the orbital phases 0.6–0.9 and 0.25–0.30. We show, in Fig. 2, the first *Resolve* spectrum of Vela X-1 collected during the observation at phase 0.6–0.9. The Figure also reports the *Chandra*/HETG spectrum collected at the same orbital phase for comparison (the normalization of the HETG spectrum is scaled up to mimic an equivalent effective area at 6 keV). The Figure confirms the energy calibration for *Resolve*.

The detailed spectral analysis of the *Resolve* data is currently underway and will provide valuable insights into various aspects of the stellar wind environment in Vela X-1. In particular, the data will shed light on how the stellar wind interacts with the gravitational field of the

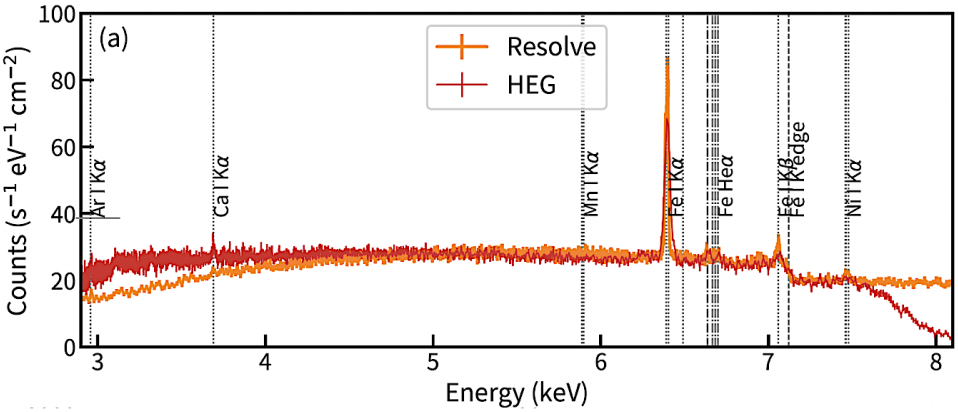

Figure 2: Stacked spectra of *Resolve* and HEG (high energy grating) in HETG divided by effective area for phase 0.6. Emission lines from neutral medium (dotted) and highly ionized plasma (dashed-and-dotted) as well as absorption edge (dashed) are shown with vertical line. The inconsistency between the two is due to different absorption column in the line of sight at the low-energy end and to an artifact of HETG data processing at the high-energy end.

compact object, and the influence of X-rays on wind ionization and structure. The elemental abundances present in the wind can be accurately determined, contributing to a deeper understanding of the system's overall chemical composition.

3.2. Centaurus X-3 (Cen X-3)

Cen X-3 is another eclipsing HMXB consisting of an O star and a pulsar spinning with a period of ~ 4.8 s [4, 12, 13]. The X-ray spectrum of the source shows a plethora of emission lines like Fe, Si, Mg and Ne [14–18]. The lines are produced in the stellar wind, which is all around the neutron star and therefore the line energy shift and width provide information about the velocity field of the line forming region. As the neutron star goes into eclipse or comes out of eclipse, during the transition region, only some parts of the line formation region will be visible. The changes in the line width, or maybe even the line centroid during the eclipse transitions, will help to determine the radial velocity structure of matter in the system.

Neutral Fe Kα fluorescence lines are ubiquitous to HMXBs and originate in the cold and dense material surrounding the compact object. In most eclipsing binaries, when the central compact object is hidden, the equivalent width of the neutral Fe Kα line is larger than in non eclipsing phases. Interestingly, though, Cen X-3 is one exception for which the equivalent width of the Fe Kα line decrease during eclipse compared to the out-of-eclipse phase while other ionized lines (Fe XXV and Fe XXVI) show the reverse trend. This implies that the ionized lines are formed in the outer regions of the binary system in the highly photo-ionized wind of the donor star or in the accretion disk corona, while there are active debates regarding the origin of Fe Kα line [14–18].

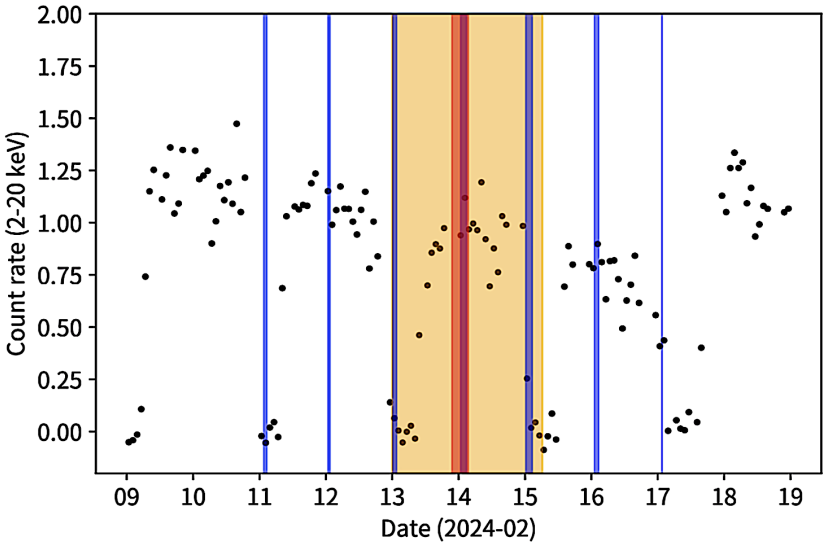

Figure 3: *MAXI*/GSM count rate in black-dots and *XRISM* observation duration is marked in orange. Also shown are *NICER* observations of Cen X-3 in blue and *NuSTAR* observation in red during *XRISM* observations.

XRISM observed Cen X-3 for one full orbit during February, 2024 as seen in Fig. 3. The black markers show the *MAXI*/GSM count-rate with the *XRISM* observation marked in the orange band. *NICER* also monitored the source around the same time and the corresponding time-coverage is shown in the same figure with blue bands. The red line on February 14, 2024 is the simultaneous *NuSTAR* observation. In Fig. 4, we show the count-rate spectrum of Cen X-3 in and out of eclipse. We find that few hundreds of seconds of exposure are sufficient to disentangle – for the first time – the lines of the Fe Kα doublet and the He-like Fe XXV fine structure, improving, in general, the determination of the plasma parameters of the source. Fitting the equivalent width of the Fe Kα line with the expectation from radiative transfer (3D Monte-Carlo simulation) using SKIRT indicates that the line emission may arise from the accretion matter between the O star and the neutron star, illuminated by non-isotropic X-ray emission from the neutron star, although emission from the hot-spot on the companion O star can also be a possibility. A detailed analysis of the *Resolve* data is presented elsewhere [19].

4. Summary

The high-resolution X-ray spectra being measured by *XRISM*/*Resolve* are transforming our understanding of a broad range of astrophysical systems, including the physics of HMXBs. With the excellent spectral resolution in the Fe K band, we can, for the first time, resolve the Fe I Kα doublet as well as the fine structure of the Fe XXV and Fe XXVI Ly α lines accurately. Thanks to the large effective area of *Resolve*, we can study the emission line shifts as a function of orbital and spin phases and changes in the line widths to determine the radial velocity field around the formation region in the surroundings of the compact object. Additionally, the ionization of the wind by the X-ray emission from the compact object is expected to affect the acceleration of the wind by the companion star's UV light. Differential line shifts within a line

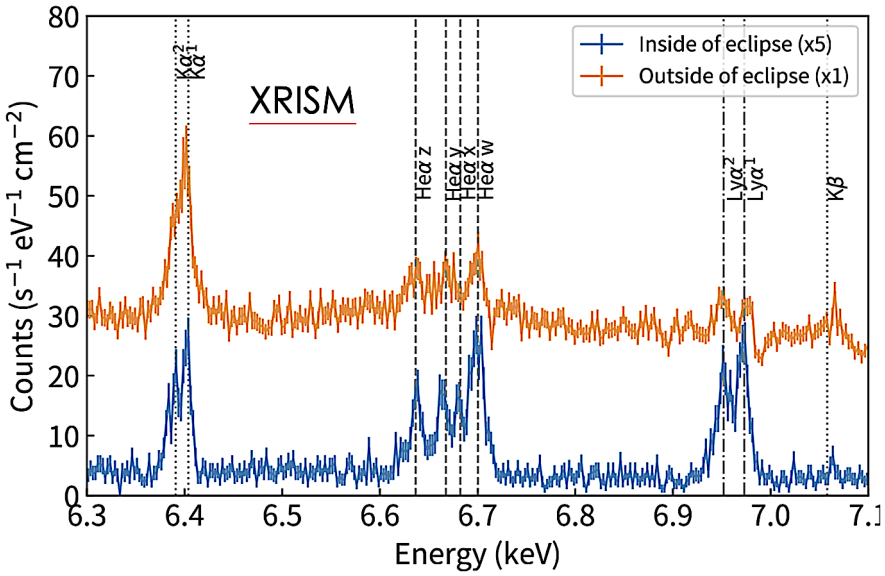

Figure 4: Count-rate spectrum of Cen X-3 in and out of eclipse exhibiting the spectral differences in the two phases.

complex will help investigate the ionization states and velocities of different regions within the binary system. Furthermore, the line profile diagnostics provide information on the physical conditions, such as temperature, density, and velocity fields of the emitting plasma offering clues about wind structures and accretion flows.

Acknowledgments

The authors thank all those who contributed to the *XRISM* mission. Camille M. Diez gave useful comments for the manuscript. This work was supported by the JSPS Core-to-Core Program (grant number: JPJSCCA20220002).

Further Information

Authors' ORCID identifiers

0000-0002-1131-3059 (Pragati PRADHAN)
0000-0002-9184-5556 (Masahiro TSUJIMOTO)

Author contributions

PP authored Sects. 3 and 4, and is involved in the analysis of Cen X-3 as a part of the XRISM team for the source. MT authored Sects. 1 and 2, and played a pivotal role in the data analysis for both Vela X-1 and Cen X-3.

Conflicts of interest

The authors declare no conflict of interest.

References

[1] Ishisaki, Y., Kelley, R. L., Awaki, H., Balleza, J. C., Barnstable, K. R., Bialas, T. G., Boissay-Malaquin, R., Brown, G. V., Canavan, E. R., Cumbee, R. S., and *56 more* (2022) Status of resolve instrument onboard X-ray Imaging and Spectroscopy Mission (XRISM). In *Space Telescopes and Instrumentation 2022: Ultraviolet to Gamma Ray*, edited by den Herder, J.-W. A., Nakazawa, K., and Nikzad, S., volume 12181. SPIE. https://doi.org/10.1117/12.2630654.

[2] Tashiro, M. S., Watanabe, S., Maejima, H., Toda, K., Matsushita, K., Yamaguchi, H., Kelley, R. L., Reichenthal, L. S., Hartz, L. S., Petre, R., and *175 more* (2024) Development and operation status of X-Ray Imaging and Spectroscopy Mission (XRISM). In *Space Telescopes and Instrumentation 2024: Ultraviolet to Gamma Ray*, edited by den Herder, J.-W. A., Nikzad, S., and Nakazawa, K., volume 13093. SPIE. https://doi.org/10.1117/12.3019325.

[3] Canizares, C., Davis, J., Dewey, D., Flanagan, K., Galton, E., Huenemoerder, D., Ishibashi, K., Markert, T., Marshall, H., McGuirk, M., Schattenburg, M., Schulz, N., Smith, H., and Wise, M. (2005) The *Chandra* high-energy transmission grating: Design, fabrication, ground calibration, and 5 years in flight. *PASP*, **117**(836), 1144–1171. https://doi.org/10.1086/432898.

[4] Chodil, G., Mark, H., Rodrigues, R., Seward, F. D., and Swift, C. D. (1967) X-Ray intensities and spectra from several cosmic sources. *ApJ*, **150**, 57–65. https://doi.org/10.1086/149312.

[5] Nagase, F., Zylstra, G., Sonobe, T., Kotani, T., Inoue, H., and Woo, J. (1994) Line-dominated eclipse spectrum of Vela X-1. *ApJ*, **436**, L1–L4. https://doi.org/10.1086/187619.

[6] van Kerkwijk, M. H., van Paradijs, J., and Zuiderwijk, E. J. (1995) On the masses of neutron stars. *A&A*, **303**, 497–501. https://ui.adsabs.harvard.edu/abs/1995A&A...303..497V.

[7] Watanabe, S., Sako, M., Ishida, M., Ishisaki, Y., Kahn, S. M., Kohmura, T., Nagase, F., Paerels, F., and Takahashi, T. (2006) X-Ray spectral study of the photoionized stellar wind in Vela X-1. *ApJ*, **651**(1), 421–437. https://doi.org/10.1086/507458.

[8] Fürst, F., Kreykenbohm, I., Pottschmidt, K., Wilms, J., Hanke, M., Rothschild, R. E., Kretschmar, P., Schulz, N. S., Huenemoerder, D. P., Klochkov, D., and Staubert, R. (2010) X-ray variation statistics and wind clumping in Vela X-1. *A&A*, **519**, A37. https://doi.org/10.1051/0004-6361/200913981.

[9] Doroshenko, V., Santangelo, A., Nakahira, S., Mihara, T., Sugizaki, M., Matsuoka, M., Nakajima, M., and Makishima, K. (2013) Footprints in the wind of Vela X-1 traced with MAXI. *A&A*, **554**, A37. https://doi.org/10.1051/0004-6361/201321305.

[10] Kretschmar, P., El Mellah, I., Martínez-Núñez, S., Fürst, F., Grinberg, V., Sander, A. A. C., van den Eijnden, J., Degenaar, N., Maíz Apellániz, J., Jiménez Esteban, F., Ramos-Lerate, M., and Utrilla, E. (2021) Revisiting the archetypical wind accretor Vela X-1 in depth: Case study of a well-known X-ray binary and the limits of our knowledge. *A&A*, **652**, A95. https://doi.org/10.1051/0004-6361/202040272.

[11] Amato, R., Grinberg, V., Hell, N., Bianchi, S., Pinto, C., D'Aí, A., Del Santo, M., Mineo, T., and Santangelo (2021) Looking through the photoionisation wake: Vela X-1 at $\phi_{\rm orb} \approx 0.75$ with *Chandra*/HETG. *A&A*, **648**, A105. https://doi.org/10.1051/0004-6361/202039125.

[12] Giacconi, R., Gursky, H., Kellogg, E., Schreier, E., and Tananbaum, H. (1971) Discovery of periodic X-ray pulsations in Centaurus X-3 from *UHURU*. *ApJ*, **167**, L67–L73. https://doi.org/10.1086/180762.

[13] Schreier, E., Levinson, R., Gursky, H., Kellogg, E., Tananbaum, H., and Giacconi, R. (1972) Evidence for the binary nature of Centaurus X-3 from *UHURU* X-ray observations. *ApJ*, **172**, L79–L89. https://doi.org/10.1086/180896.

[14] Iaria, R., Di Salvo, T., Robba, N. R., Burderi, L., Lavagetto, G., and Riggio, A. (2005) Resolving the Fe XXV triplet with *Chandra* in Centaurus X-3. *ApJ*, **634**(2), L161–L164. https://doi.org/10.1086/499040.

[15] Tugay, A. V. and Vasylenko, A. A. (2009) XMM-Newton observations of X-ray pulsar Cen X-3. In *Young Scientists 16th Proceedings*, edited by Choliy, V. Y. and Ivashchenko, G., pages 58–61. https://doi.org/https://doi.org/10.48550/arXiv.0912.3354.

[16] Naik, S. and Paul, B. (2012) Investigation of variability of iron emission lines in Centaurus X-3. *BASI*, **40**(4), 503–514. http://www.ncra.tifr.res.in:8081/~basi/12Dec/503402012.pdf.

[17] Aftab, N., Paul, B., and Kretschmar, P. (2019) X-ray reprocessing: Through the eclipse spectra of high-mass x-ray binaries with xmm-newton. *ApJS*, **243**(2), 29. https://doi.org/10.3847/1538-4365/ab2a77.

[18] Sanjurjo-Ferrín, G., Torrejón, J. M., Postnov, K., Oskinova, L., Rodes-Roca, J. J., and Bernabeu, G. (2021) X-ray variability of the HMXB Cen X-3: evidence for inhomogeneous accretion flows. *MNRAS*, **501**(4), 5892–5909. https://doi.org/10.1093/mnras/staa3953.

[19] Mochizuki, Y., Tsujimoto, M., Kelley, R. L., Vander Meulen, B., Enoto, T., Nagai, Y., Done, C., Pradhan, P., Hell, N., Pottschmidt, K., Ebisawa, K., and Behar, E. (2024) Detection of the orbital modulation of Fe Kα fluorescence emission in Centaurus X-3 using the high-resolution spectrometer Resolve on board XRISM. *ApJL*, **977**(1), L21. https://doi.org/10.3847/2041-8213/ad946d.